A CORRELATION STUDY AMONG SEISMIC MONITORING, PSEUDO-DYNAMIC TEST, AND NUMERICAL SIMULATION OF INELASTIC RESPONSES OF STEEL BRACED FRAME MODEL

Seung-Jae LEE[1], Kenichi OHI[2], Yosuke SHIMAWAKI[3] And Hideo KONDO[4]

SUMMARY

This paper presents a series of substructuring pseudo-dynamic tests on steel brace members in order to simulate the real inelastic responses of the steel braced frame monitored during moderate earthquakes. A pair of brace members at the first story were chosen as substructure specimens for loading tests. As for other fictitious portions, linear-elastic behavior was assumed, and the whole system was solved as a shear-type 3-DOF planar system. Monitored responses and the test results are also compared with completely numerical response analysis using a mathematical model for brace members.

INTRODUCTION

By means of numerical response analysis, we can predict inelastic behaviors of structural system during severe earthquakes. The responses simulated are, however, greatly influenced by the appropriateness of the constitutive mathematical models for structural elements and system. To discuss the validity of the mathematical models, real inelastic responses of a real structure are desired to be collected. On such a motivation, a seismic monitoring project was begun since 1984 on model structures including a steel braced frame model with intentionally reduced seismic strength at Chiba in Japan [K. Takanashi et al.,1985]. Another technique to simulate seismic responses, not real but close to real, is a pseudo-dynamic simulation based on computer-controlled loading tests on structural elements or a whole structural system. In this paper, to study how accurately the hybrid test technique of this kind can simulate real responses, a series of substructuring pseudo-dynamic tests are carried out. In the testing, the real inelastic responses of the steel braced frame during three moderate events are simulated by the substructuring pseudo-dynamic tests. First this paper presents a summary of three monitoring events. Next a series of substructuring pseudo-dynamic tests and completely numerical response analysis are performed on three-story braced frame model to compare with the real responses monitored.

SUMMARY OF EARTHQUAKE RESPONSE MONITORED

The shapes and dimensions of the model structure are shown in Figs. 1 and 2, and the fundamental parameters are summarized on Table 1. Typical three events are chosen for the comparison in this study and their peak

acceleration responses are summarized on Table 2. As for the first two events, almost the same peak ground acceleration (abbreviated to PGA), about 70 gals, were felt at the observation site. The brace members were damaged moderately (ductility responses were about 3 through 5) at the first story commonly by these two events, but the number of yield reversals were considerably different. During the third event about 300 gals in

[1] *Institute of Industrial Science, University of Tokyo, Tokyo, Japan Email: leeseung@cc.iis.u-tokyo.ac.jp*
[2] *Institute of Industrial Science, University of Tokyo, Tokyo, Japan*
[3] *Institute of Industrial Science, University of Tokyo, Tokyo, Japan*
[4] *Institute of Industrial Science, University of Tokyo, Tokyo, Japan*

PGA was felt, and this was the largest event in the project: The brace members were severely damaged at the first story, and also the columns and the connections in the transverse direction were also slightly damaged.

To determine dynamic properties including damping of model structure, we identified the system gain from input-output records monitored by fast Fourier Transform (FFT) technique. The process of system identification is as follows: First the fast Fourier transform of input acceleration at basement and that of output acceleration monitored at roof are executed. Second the energy spectrum of input record and the cross spectrum of input and output records are calculated. Third the computed spectral values, the energy spectrum and the cross spectrum, are smoothed by a rectangular window, the bandwidth of which is set to 0.3Hz. Then we can identify the system gain by the quotient of two spectral values.

The theoretical system gain given Eq.(1) is compared with the system gain identified by the above-mentioned spectral processing. And we evaluated mass of each floor by the dimension of model structure and adopted the values of initial stiffness of each floor as ones derived from the monitored shear vs. drift curves of each floor.

$$ {}_j H(\omega) = 1 + \sum_{S=1}^{3} \frac{{}_j\phi_S \cdot \omega^2}{{\omega_S}^2 - \omega^2 + 2h_S \cdot \omega_S \cdot \omega \cdot i} \tag{1} $$

Where, ${}_j\varphi_S$ is participation vector of S^{th} mode, j^{th} floor, ω_S is natural frequency of S^{th} mode, n_S is damping factor of S^{th} mode.
Therefore we can evaluate the first modal damping factor by the above-mentioned process. But we assumed the second and the third mode damping factors as external viscous damping (mass-proportional damping) because the peaks of system gain identified at the two natural frequency are not clear in comparison with that of the first mode.
The results of dynamic properties evaluated are shown in Tables 3. and 4. The system gain identified and the theoretical system gain based on Eq. (1) with the assumption of external viscous damping are shown in Fig.3. In order to check the accuracy of the dynamic properties identified, elastic response analysis are performed on a shear-type 3-DOF planar system. As shown in Fig.4, the responses of analysis using dynamic properties evaluated have a good agreement with the response monitored within elastic limit.

SUBSTRUCTURING PSEUDO-DYNAMIC TESTS

Procedure of Simulation

A series of substructuring pseudo-dynamic tests were performed with the base acceleration records monitored during these three events. In the testing, a pair of brace members at the first story were chosen as substructure specimens for loading tests. As for other fictitious portions, linear-elastic behaviors were assumed, and the whole system was solved as a shear-type 3-DOF planar system as shown in Fig.5. The equation of motion is:

$$ [M]\{\ddot{X}\} + [C]\{\dot{X}\} + [K]\{X\} + \{R\} = -[M]\{1\}\ddot{y} \tag{2} $$

Where, $[M] = \begin{bmatrix} m_1 & & \\ & m_2 & \\ & & m_3 \end{bmatrix}$, $[K] = \begin{bmatrix} k_F + k_2 + k_{P\Delta} & -k_2 & \\ -k_2 & k_2 + k_3 & -k_3 \\ & -k_3 & k_3 \end{bmatrix}$, $\{R\} = \begin{Bmatrix} R_1 \\ 0 \\ 0 \end{Bmatrix}$

Assuming proportional damping, [C] is determined using the evaluated damping factors and the natural frequencies. Stiffness of the first floor, k_F, and additional stiffness due to P-Δ effect, $k_{P\Delta}$, are evaluated by following formula:

$$ k_F = \frac{12E \cdot I}{H^3} \cdot 4 \tag{3} $$

$$k_{P\Delta} = -\sum_{j=1}^{3} \frac{m_j \cdot g}{H} \tag{4}$$

Where, *E* is Young's modulus, *I* is moment of inertial of the column section, and *H* is the height of floor. k_2 and k_3 are set to the values on Table 3. R_1 is the restoring force of the pair of brace members of the first floor, which are tested in the loading test. Other brace members are assumed elastic and already included in the stiffness, k_2 and k_3. $\{\ddot{X}\}, \{\dot{X}\}$, and $\{X\}$ are acceleration, velocity, and displacement relative to ground motion, respectively. $\ddot{y}$ is the acceleration monitored at the basement.

The central difference method is utilized for numerical integration of the response analysis. In the procedure of the testing, when loading of i^{th} step is completed and put forward to $i+1^{th}$ step, $\{X\}_{i+1}$ can be calculated from Eq.(5).

$$\{X\}_{i+1} = [M] + \frac{\Delta t}{2}[C] - \Delta t^2([M]\{1\}\ddot{y} - \{R\}_i - [K]\{X\}_i + \frac{\Delta t}{2}[C]\{X\}_{i-1} - [M]\{X\}_{i-1} + 2[M]\{X\}_i \tag{5}$$

If the brace members directly connected to the nodes of frame, then the target displacement to be applied to the pair of brace specimens can be calculated simply from $\{X\}_{i+1}$ by geometric relation. However, in the model structure, brace members are connected to the frame node via the gusset plate and angle pieces in series. That is, target displacement consists of including not only a pair of brace specimens deformations but also deformations of other elements. In the loading test, only a pair of brace members are to be loaded. The deformation of other elements are evaluated by the restoring force of brace specimens, and considered in the control of specimen displacements. Satisfying the condition, Eq.(6), loading of $i+1^{th}$ step is regarded as completed.

$$\left(X_i - X_{i+1}\right) \cdot \left(\delta_m + \frac{F_m}{2k_a} - \delta_{i+1} \right) \leq 0 \tag{6}$$

Where, δ_m is the measured axial displacement of specimens, δ_{i+1} is the target axial deformation for the series system of specimens and other elements in the $i+1^{th}$ step, where F_m and k_a are the measured axial force of brace specimens and the stiffness of gusset plate and angle pieces, respectively. The brace members are made of ordinary mild steel, JIS SS400 grade as shown in Fig.6, and test setup is shown in Fig.7.

Tests results and comparison with numerical analysis

Completely numerical simulation was performed on the basis of mathematical model for brace members [M. Shibata et al. , 1982]. Other analysis conditions are the same as those of substructuring pseudo-dynamic test. Responses of hysteresis loops and displacements are plotted in Figs. 8 and 9. The overall inelastic responses of the tests and monitored results agree with sufficient accuracy. But tested and monitored peak response values are different slightly. It is due to discrepancy between the material properties of tested brace specimens and brace members of model structure. As for the two moderate events, the substructuring pseudo-dynamic tests successfully simulated the process of inelastic responses with sufficient accuracy. As for the severe event, small discrepancy in the hysteresis loop at the first story was found due to the simplicity of the shear-type planar system assumed, but the magnitudes of peak responses were well simulated.

To examine the relation between damage distribution of model structure and damage potential of earthquake, Energy Input Rate Spectrum (abbreviated to EIR spectrum, [K.Ohi et al., 1991]) of monitored response, tested response, and acceleration for input, are calculated and shown in Fig.10. The two earthquakes have almost the same peak values of PGA but the distribution of damage potential is different in both of them. Earthquake monitored on October 4, 1985 has impulse-like damage potential as shown in Fig. 10(a) and predominant frequency of response changed suddenly after yielding as shown in Fig. 10(b). On the other hand, earthquake monitored on June 24, 1986 has long lasting damage potential as shown in Fig. 10(d) and the predominant frequency changed slowly as shown in Fig. 10(e). In the EIR spectra, the change of predominant frequencies between the simulated responses and the monitored responses agree fairly well.

CONCLUDING REMARKS

It is demonstrated through the comparison with real response process monitored that the substructuring pseudo-dynamic test technique provides an efficient experimental tool for prediction and simulation of real inelastic behaviors during earthquakes, so far as an appropriate substructure and an appropriate system modeling are chosen.

REFERENCES

K. Ikeda, K. Ohi, K. Takanashi, X.G. Lin (1997), "Response observation and substructuring on-line test for weekly designed steel structure models," Annual meeting of the AIJ, Structure F , pp807-808

K. Ohi, K. Takanashi, Y. HOMMA (1991), "Energy input rate spectra of earthquake ground motions", Journal of Structural Construction Engineering, AIJ, No.420, pp1-7

K. Takanashi, K. OHI, X. GAO (1985), " Response and failure observation of weakly designed steel structure models (Part 1)", Bulletin of ERS, IIS, Univ. of Tokyo, No.18, pp39-47

M. Shibata, T. Nakamura, M.Wakabayashi (1982), " Mathematical expression of hysteretic behavior of braces (Part 1 Derivation of hysteresis function)", Journal of Structural Construction Engineering, AIJ, No.316, pp18-24

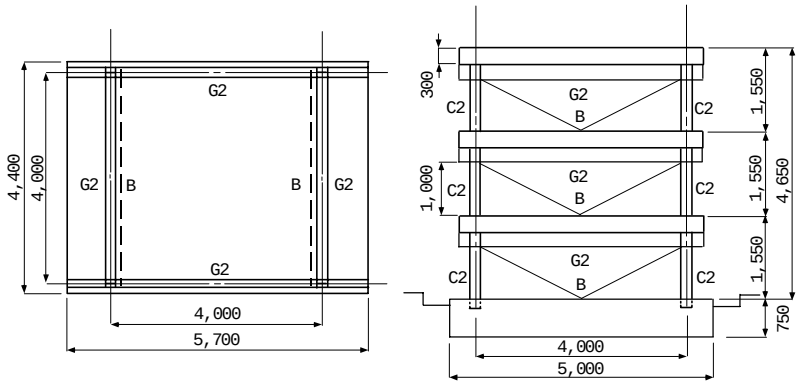

(a) Plan **(b) Elevation**

Figure 1: Dimensions of model structure

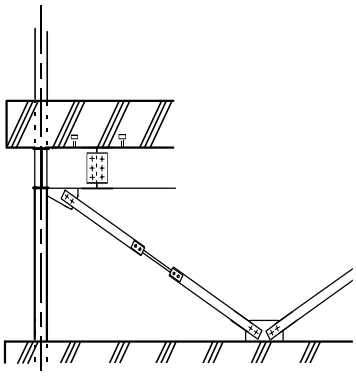

Figure 2: Details of brace member

Table 1: Parameters of model structure

Stories		3
Area of floor		25.1m^2
Weight of each floor	1Fl.	18.8 t
	2Fl.	18.8 t
	3Fl.	18.4 t
Steel grade		JIS SS 400
Steel members	C2	H-700×50×5×7
	G2	H-250×75×6×6
	B	PL-6×9
	Additional brace	L-65×65×6

Table 2: Peak values of monitored responses

Date	N. Lat.	Magnitude	Axis	Peak values of acceleration(gal)			
Time	E. Long.	Depth		Base	1Fl.	2Fl.	3Fl.
1985.10.04	N35°53′	M6.0	X	39.5	170.7	88.0	165.1
21:26	E140°09′	78km	Y	74.3	132.9	259.4	352.2
1986.6.24	N34°08′	M6.9	X	73.7	167.9	140.5	185.6
11:53	E140°08′	80km	Y	54.6	132.3	248.2	341.0
1987.12.17	N35°2?	M6.7	X	167.1	184.1	167.4	198.4
11:08	E140°29′	58km	Y	301.4	419.7	550.3	741.1

X: Weak-axis direction of H-shaped column section Y: Strong-axis direction of H-shaped column section

Table 3: Mass and stiffness

Floor	Mass(ton*sec^2/cm)	Stiffness(ton/cm)
1	0.0192	34.5
2	0.0192	48.4
3	0.0188	48.5

Table 4: Dynamic properties

Mode	Natural frequency(Hz)	h_i(%)
1st	3.22 (3.23)	1.53
2nd	10.06 (9.49)	0.49
3rd	15.04 (14.24)	0.33

Where, the values put in parentheses are calculated from the system identification.

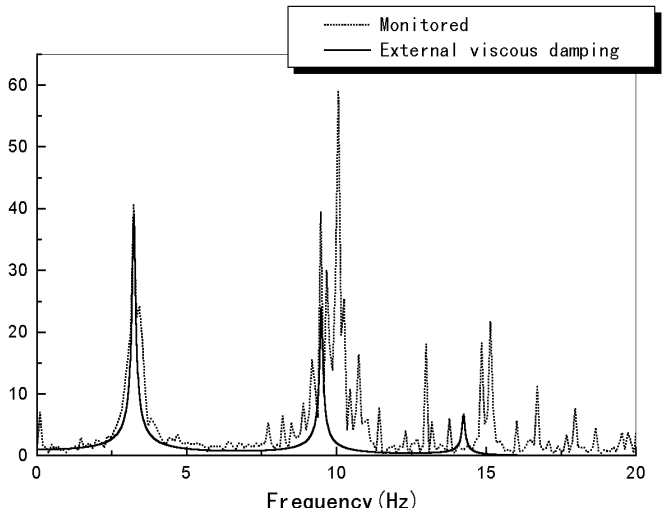

FIGURE 3: SYSTEM GAIN

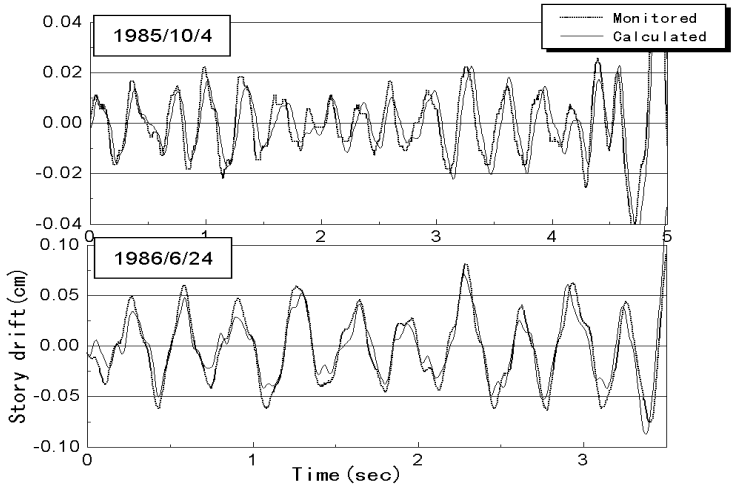

FIGURE 4: TIME HISTORY OF STORY DRIFT OF THE FIRST FLOOR

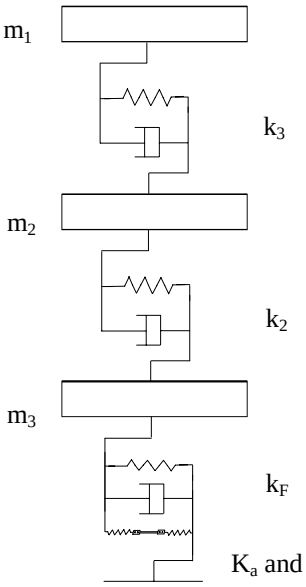

FIGURE 5: ANALYZED VIBRATION MODEL

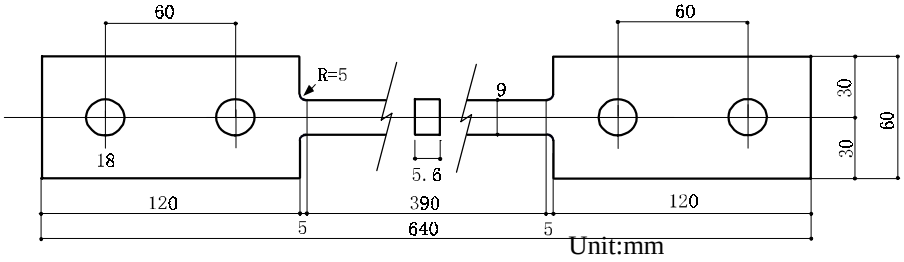

FIGURE 6: DIMENSIONS OF BRACE SPECIMEN

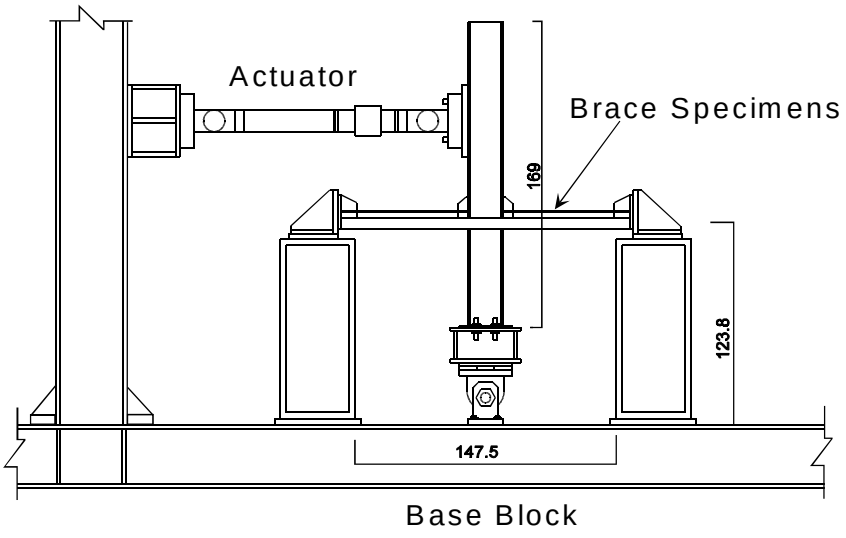

FIGURE 7: TEST SETUP

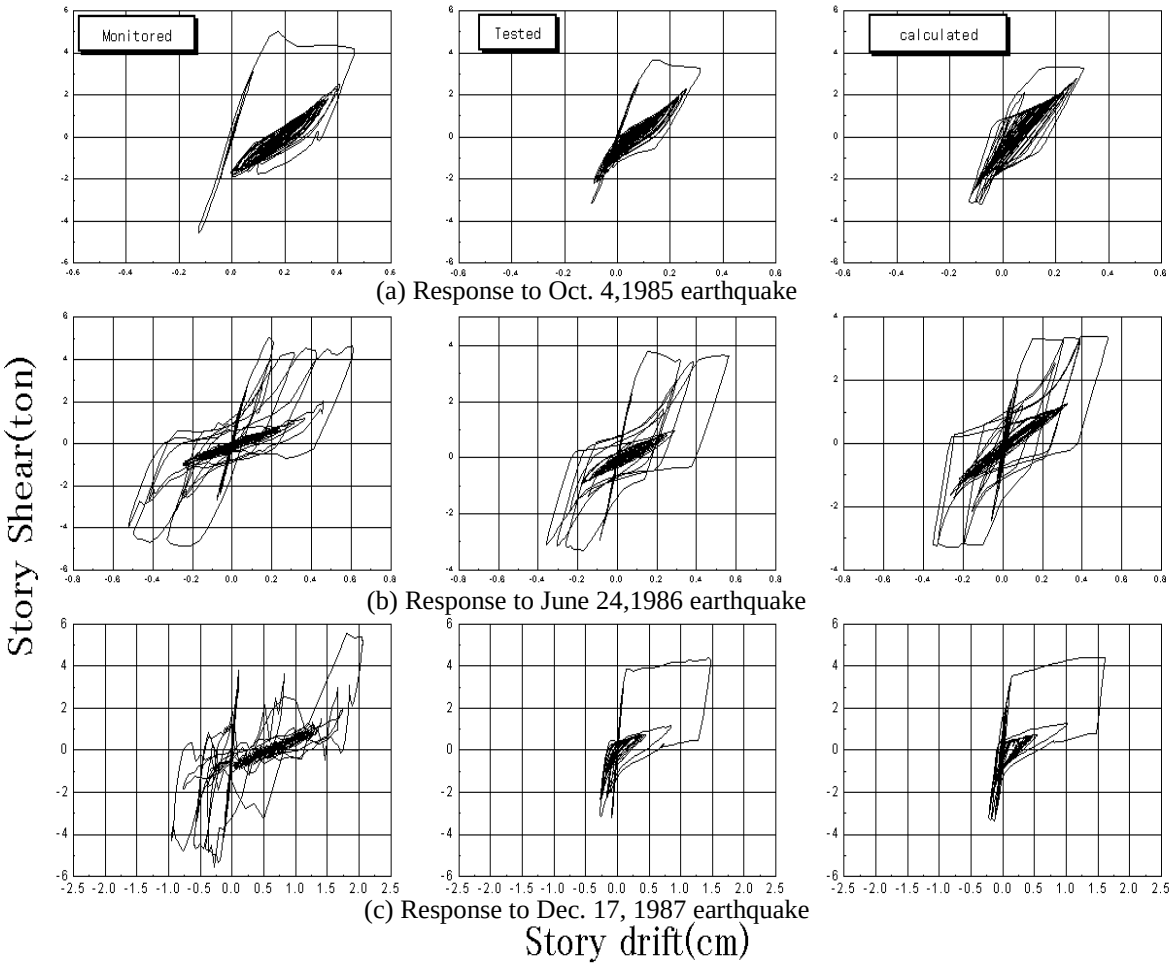

FIGURE 8: HYSTERESIS BEHAVIOR AT THE FIRST STORY

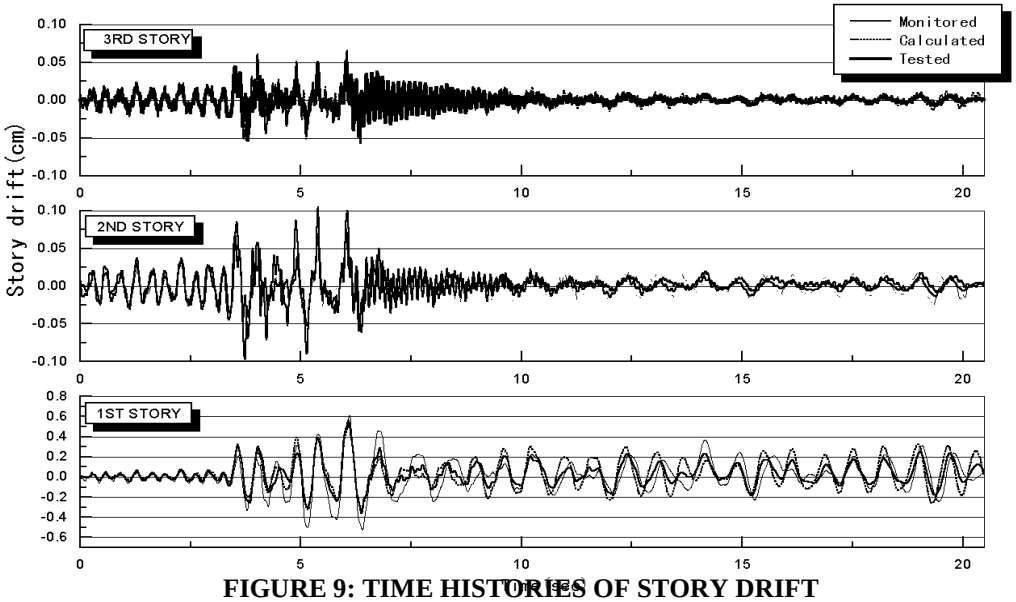

FIGURE 9: TIME HISTORIES OF STORY DRIFT

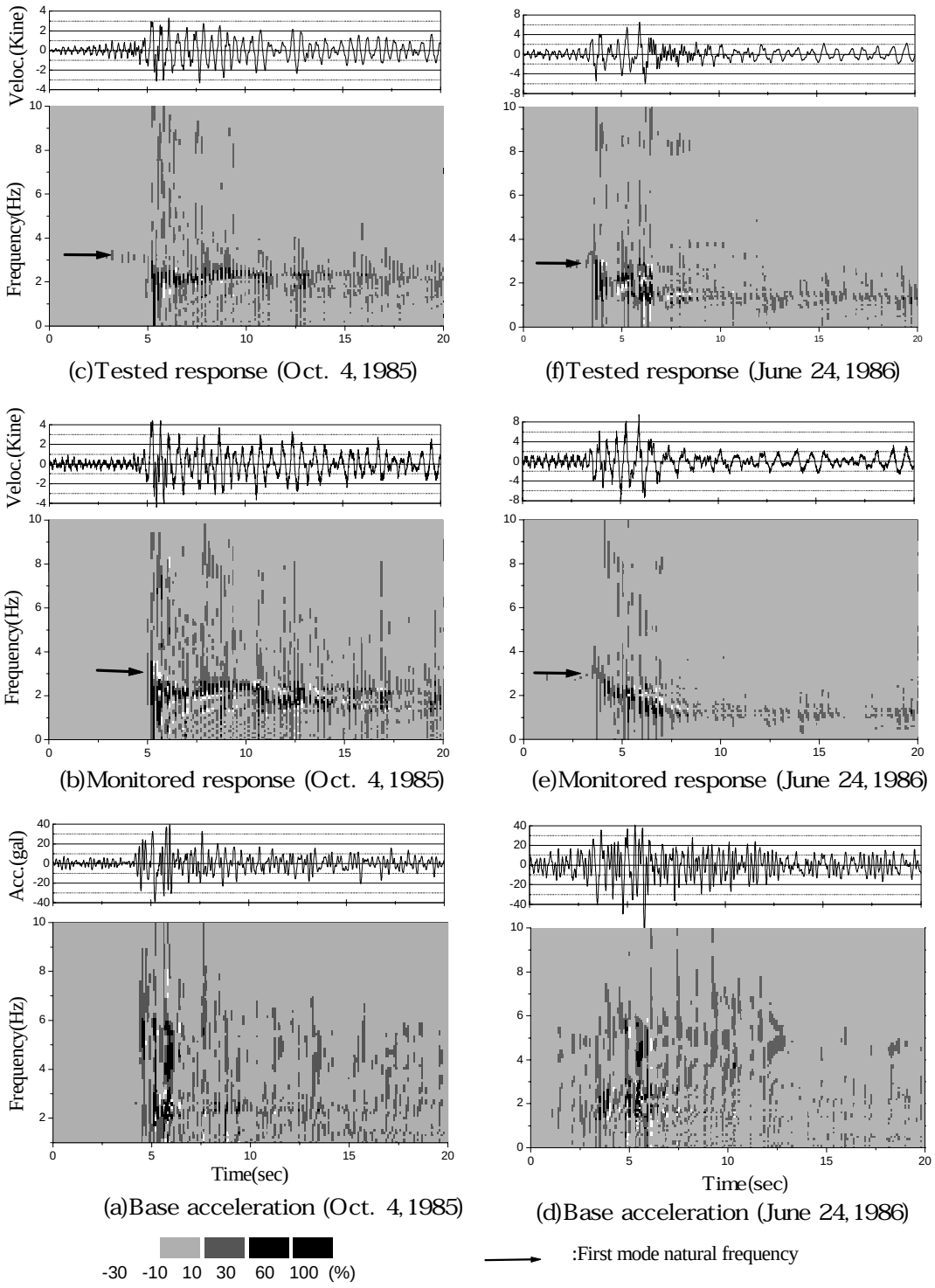

FIGURE 10: EIR SPECTRA OF BASE ACCELERATION, MONITORED RESPONSE, AND TESTED RESPONSE